SAR Distribution and Temperature Increase in an Anatomical Model of the Human Eye Exposed to the Field Radiated by the User Antenna in a Wireless LAN

Paolo Bernardi, *Fellow, IEEE*, Marta Cavagnaro, Stefano Pisa, *Member, IEEE*, and Emanuele Piuzzi

***Abstract*— Wireless personal communication is a rapidly expanding sector, particularly in the field of cellular mobile phones and wireless local area networks (WLAN's). In an indoor WLAN system, the user of the mobile terminal can find himself in close proximity to the radiating antenna. It is, therefore, important to consider possible health hazards due to this type of exposure. As the most considered adverse effects of the electromagnetic (EM) fields are of thermal nature, particularly with reference to the eye, in this paper, we have evaluated the temperature increase induced in a human eye exposed to WLAN-like fields. In particular, we have considered possible WLAN's operating in the range between 6–30 GHz, so that the incident field can be simulated via a plane wave. As a first step, we have computed the specific absorption rate (SAR) distribution in a human-eye anatomical model, developed from the "visible human" data set, by using the finite-difference time-domain (FDTD) numerical technique with a cell resolution of 0.5 mm. Starting from the calculated SAR values, the heating distribution has been derived through the bioheat equation, which has been solved using an explicit finite-difference scheme. Temperature increases in the order of 0.04 $^{\circ}$C have been calculated in the eye lens with an incident power density of 1 mW/cm^2 at 6 GHz. Lower heating is obtained in the lens when the frequency increases. Finally, considerations about the exposure limits in the considered frequency range are made.**

***Index Terms*— Biological effects of electromagnetic radiation, dosimetry, electromagnetic heating, FDTD methods, temperature, wireless LAN.**

I. Introduction

INDOOR applications of wireless local area networks (WLAN's) were introduced in the early 1980's to reduce the installation and relocation costs of conventional wired local area networks (LAN's) and to allow the mobility of connected elements in the work space [1]. The existing applications of WLAN's are unlicensed spread-spectrum systems operating the industrial, scientific, and medical (ISM) frequencies around 2.45 and 5.8 GHz, and licensed cellular systems operating at 18–19 GHz. More recent WLAN's projects contemplate the use of millimeter-wave frequencies (30 and 60 GHz) [2]. In fact, in this frequency region, wide bands are still available from spectrum regulatory agencies, and the signal is more confined within rooms or buildings, thereby increasing the possibility of frequency reuse and the privacy of communications.

To transmit data, wireless LAN systems use a directive antenna placed at a mobile personal terminal (computer, telephone, camera, etc.) and a wide beam antenna placed at a fixed site (the base station) usually located at the room ceiling or high on a vertical wall. In this arrangement, the user can find himself in close proximity to the radiating mobile antenna, where the electromagnetic (EM) field assumes its highest values. In particular, the user is exposed to an EM field made of the wave directly coming from the radiating antenna and waves produced by reflection and scattering from objects present in the area. As a consequence, it is important to consider the possible health hazard due to such systems and, in particular, to define the EM field values that are safe for human beings.

With reference to the kind of applications under consideration, the frequency range around 2.45 GHz has already been sufficiently investigated due to its extensive use in ISM applications. In this paper, therefore, we specifically focused our attention on the frequency range between 6–30 GHz.

Over 6 GHz, the correlation between the power-flux density of the incident field and the specific absorption rate (SAR) inside the exposed body has usually been obtained by using geometrical optics [3]. This technique assumes the incident field wavelength very short in comparison with the dimensions of the exposed region of the body, so as to describe the incident radiation by rays. The body is usually modeled as a sphere or prolate spheroid, and the additional approximation is made that internal absorption is high enough for the rays not to be internally reflected, but completely absorbed.

In this frequency range, the eye seems to be one of the most hazardously exposed body organs. In fact, the absorption takes place mainly in the skin, and the eye, at least when eyelids are open, is not protected by a skin layer. The above-mentioned assumptions seem not to be appropriate in the study of the exposure of the human eye. In fact, due to the eye's strongly inhomogeneous physical structure and to its reduced dimensions (compared to wavelength), geometrical optics is not applicable. Moreover, the eye is an organ particularly sensitive to heating because of the lack of blood flowing into it, and it is subject to thermal damage (lens cataract) even in the presence of weak heating.

Manuscript received December 3, 1997; revised August 1, 1998. This work was supported by the Italian National Research Council (CNR) under Contract S774-WWLAN.

The authors are with the Department of Electronic Engineering, University "La Sapienza" of Rome, 00184 Rome, Italy (e-mail: bernardi@die.ing.uniromal.it).

Publisher Item Identifier S 0018-9480(98)09044-9.

On the basis of the previous observations, we have performed a theoretical study of the heating induced inside the human eye exposed to fields with frequencies greater than 6 GHz. The analysis has been conducted using an accurate anatomical model of the human eye and of surrounding cranial structures and utilizing finite-difference techniques to solve both the EM and thermal problem. In particular, we have evaluated SAR absorbed in the eye using the finite-difference time-domain (FDTD) algorithm. Starting from SAR distribution, we have computed the induced heating by solving the bioheat equation with an explicit finite-difference scheme.

The majority of the studies conducted on the eye exposure to microwave fields, both experimentally and theoretically, has concerned the ISM frequencies of 915 MHz and 2.45 GHz.

As concerns the experimental studies because of the difficulty in performing experiments directly on the human eye, investigators have worked with rabbits, having an eye anatomical structure similar to that of the corresponding human organ. The first detrimental effect evidenced by these experiments has been lens cataract [4]. Many experiments, performed at frequencies around 2.45 GHz evidenced that an incident power density higher than 100 mW/cm^2 lasting at least 30 min, can induce lens opacification (cataract) [4]. These experiments also demonstrated that the threshold for the induction of the cataract depends on the product of the incident power density with the exposure time. In particular, the higher the power, the smaller the exposure time necessary to induce lens cataract. According to the authors of these experiments, this is the main proof of the fact that lens cataract is a thermal effect [4].

Guy *et al.* [5] measured the temperature inside the rabbit eye during 2.45-GHz irradiation and found a thermal threshold for the induction of cataract equal to 41 °C, corresponding to a temperature increase of about 3 °C (the rabbit's blood temperature is about 38 °C). Experiments on other animals (e.g., dogs [6]) have confirmed a threshold of 3 °C heating in the lens for the induction of the cataract. Extrapolating these data to the human eye, the minimum temperature to be reached to induce lens opacification should be of about 40 °C.

All mentioned experiments concentrated on the investigation of possible thermal effects on the lens. This is justified by the fact that at frequencies around 2.45 GHz, the EM radiation penetrates sufficiently deep in the eye, so that the part of the eye most at risk is its inner region. However, when moving toward higher frequencies (6–30-GHz range), the EM radiation has a smaller penetration depth and, therefore, a great power deposition takes place directly in the cornea, which becomes another hazardously exposed tissue [7]. Unfortunately, its thermal sensitivity has not been extensively investigated. Anyhow, as this tissue is very similar to skin, the temperature increase necessary to induce thermal damage should be at least 10 °C [8], [9].

In addition to the above cited experimental works, some theoretical studies have been performed in order to evaluate SAR distribution and the induced heating in an exposed eye. One study, conducted by Taflove and Brodwin [10], considered the interaction of a model of the human eye with 750-MHz and 1.5-GHz radiations, both from a dosimetric and a thermal point-of-view. With an incident power density equal to 100 mW/cm^2, they found a temperature hot spot of 40.4 °C in the lens. Similar values have been measured by Guy *et al.* in the rabbit's eye irradiated at 2.45 GHz with the same power density [5].

Many international protection organizations and regulatory agencies have proposed recommendations for a safe exposure. The most commonly recognized are the IEEE C95.1-1992 Standard [11], the INIRC/IRPA 1988 Guidelines [12], and the European Committee for Electrotechnical Standardization (CENELEC) Prestandard ENV 50 166-2 [13].

Among the above mentioned standards, and with reference to the general population, the most stringent limit in the 6–30-GHz range is 1 mW/cm^2 [13]. This value should guarantee that, in any part of the exposed body, the basic limit on the local SAR (2 W/kg averaged over any 10 g of tissue) is never exceeded. On the contrary, the most relaxed limit for the incident power density is 10 mW/cm^2 [11].

When studying the interaction from a thermal point-of-view, it would be useful to have limits directly involving temperature increase in the tissues. On the basis of the previously reported experimental data, considering a safety factor of ten on the temperature increase (equal to that adopted on the SAR), the maximum acceptable temperature increase should be 0.3 °C in the lens and 1 °C on the cornea. These are the threshold values that we have used in our work to judge the "safety" of exposure from the thermal point-of-view.

II. Methods and Models

A. Head Model

The head model has been obtained from photographic images of the human head. These images have been taken from the "visible human project" data set representing an internationally known anatomic data base.[1]

To obtain an FDTD-compatible head model, each pixel of the photographic images has been converted into an integer number representing the corresponding tissue [14]. For obtaining a good accuracy of the EM solution with the FDTD method, a cell dimension of 0.5 mm has been used [14], [15].

In particular, in our simulations, two anatomical models have been used. The first is a two-dimensional model, consisting of a horizontal section of the whole head at the level of the eye (with open eyes) [see Fig. 1(a)]; the second is a three-dimensional model, and takes into account the whole eye and some surrounding anatomical structures (like the nose). The reason for including the nose in the three-dimensional model will be justified in the following. The three-dimensional model is 62-mm large, 52-mm deep, and 58-mm high. A central horizontal section of the three-dimensional model is shown in Fig. 1(b).

B. The FDTD Method

The dosimetric problem has been solved by using the FDTD technique [16], [17]. The excitation field has been supposed to have the characteristics of a plane wave. Into the FDTD method, this condition has been simulated by dividing the whole volume under study in a total field region and in a

[1] See Internet site: http://www.nlm.nih.gov.

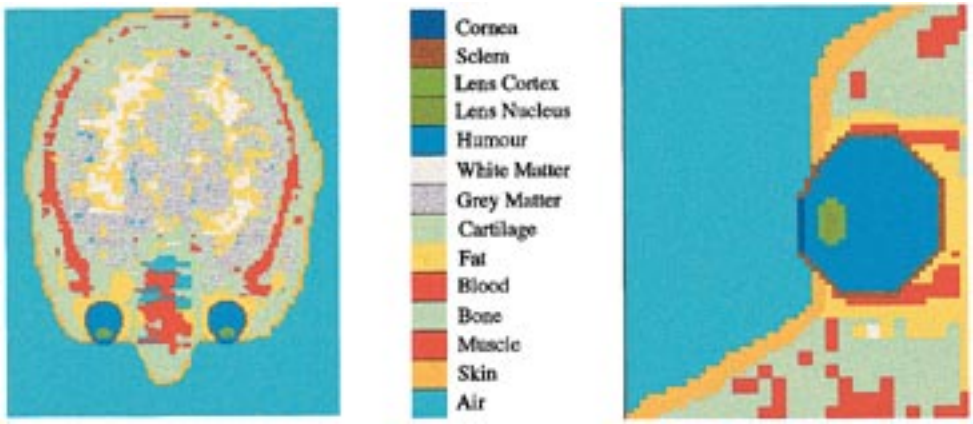

(a) (b)

Fig. 1. Anatomical models. (a) Two-dimensional model. (b) Three-dimensional model (horizontal section).

scattered field region, and by applying on the surface of the total field region a time-harmonic source field. Then, in order to bound the domain under study, the scattered field region has been closed by applying a second-order absorbing boundary condition [16], [17].

C. Electrical Parameters

Due to the lack of experimental data at the considered frequencies, the evaluation of the complex permittivity values related to the eye tissues is not straightforward. To solve this problem, we have extrapolated the permittivity values of interest to our work from experimental data available at lower frequencies and by using the Debye's dispersion equation [14], [15]. Debye's equation gives the complex permittivity (ε^*) of a dielectric material as a function of the frequency (f), according to

$$\varepsilon^*(f) = \varepsilon'(f) + \frac{\sigma(f)}{j2\pi f\varepsilon_0} = \varepsilon_\infty + \frac{\sigma_S}{j2\pi f\varepsilon_0} + \frac{\varepsilon_S - \varepsilon_\infty}{1 + j\,\dfrac{f}{f_r}} \quad (1)$$

where f_r is the γ relaxation frequency, $\varepsilon_S - \varepsilon_\infty$ is the change in the permittivity due to this relaxation process, and σ_S and ε_∞ are the limits of the conductivity at very low frequencies and of the permittivity at very high frequencies, respectively.

With reference to the head's tissues, Debye's parameters are directly available only for the lens cortex and lens nucleus [18]. However, it has been shown that for high water-content tissues, there is a linear dependence of these parameters from the water content of the tissue [19]. Starting from the values measured in the lens cortex and in the lens nucleus, and using the water content of the various tissues [18]–[21], it has been possible, by means of a simple linear interpolation, to calculate Debye's parameters for all soft tissues present in the head. The Debye's parameters of the fat and bone do not follow the above mentioned linear dependence, due to their low water content. Consequently, for these two tissues, the ε_S and σ_S values have been assumed equal to the ε' and σ values measured at about 1 GHz [19]. For all the considered tissues, the relaxation frequency f_r has been evaluated by using a linear interpolation, and ε_∞ has been assumed equal to 5.1, which is the pure-water high-frequency limit [18]. The values obtained using the above described procedure are shown in Table I. Inserting these parameters in (1), the permittivity (ε_r) and conductivity (σ) values for the various head tissues at the frequencies of interest have been obtained (see Table II). These values are comparable (within 20%) with those evaluated in [22]. Analysis of data in Table II shows that both ε_r and σ increase with tissue water content.

TABLE I
DEBYE'S PARAMETERS AND DENSITY OF THE HEAD'S TISSUES

Tissue	Water [%]	f_r [GHz]	ε_s	σ_s [S/m]	ρ [kg/m^3]
Humor	90	24.3	65.7	1.57	1000
Grey Matter	82	22.8	53.5	1.38	1050
Lens Cortex	77	21.9	45.8	1.26	1050
Sclera/Cornea	75	21.5	42.7	1.21	1050
Muscle	74	21.3	41.2	1.19	1050
Blood	74	21.3	41.2	1.19	1050
White Matter	73	21.2	39.7	1.16	1050
Skin	68	20.2	32.0	1.04	1000
Lens Nucleus	62	19.1	22.8	0.90	1050
Fat	9	9.21	10.0	0.05	1000
Bone	9	9.21	10.0	0.05	1200
Cartilage	9	9.21	10.0	0.05	1000

TABLE II
ELECTRICAL PARAMETERS OF THE HEAD'S TISSUES AT THE FREQUENCIES OF INTEREST

		6 GHz		18 GHz		30 GHz	
Water [%]	Tissue	ε_r	σ [S/m]	ε_r	σ [S/m]	ε_r	σ [S/m]
90	Humor	62.2	6.27	44.2	30.6	29.1	51.0
82	Grey Matter	50.4	5.35	34.9	24.9	22.8	40.2
77	Lens Cortex	43.0	4.72	29.4	21.2	19.2	33.6
75	Sclera/Cornea	40.0	4.46	27.2	19.7	17.9	30.9
74	Muscle/Blood	38.5	4.33	26.2	19.0	17.2	29.6
73	White Matter	37.1	4.18	25.2	18.2	16.6	28.3
68	Skin	29.8	3.49	20.1	14.4	13.5	21.8
62	Lens Nucleus	21.2	2.59	14.5	9.73	10.2	14.3
9	Fat/Bone/Cartilage	8.54	0.797	6.12	2.04	5.52	2.34
-	Air	1	0	1	0	1	0

D. The Bioheat Equation

The heating profiles inside the irradiated eye have been evaluated making use of the bio-heat equation [23]

$$K\nabla^2 T + A_0 + Q_v - B(T - T_b) = C\rho\,\frac{\partial T}{\partial t}\ [\mathrm{W/m^3}]. \quad (2)$$

This equation simply equals the heat accumulated per unit time and per unit volume in the body to the temperature increase per unit time multiplied by the thermal capacitance of 1 m^3 of tissue, given by the product between the specific heat C [J/(kg °C)] and the tissue density ρ [kg/m^3].

In particular, the four terms in the first member of (2) represent different ways through which heat is accumulated inside the tissue, precisely: 1) heat transfer through internal conduction (K [J/(s m °C)] is the thermal conductivity); 2) metabolic heat production (A_0 [J/(s m^3)]); 3) heat deposition due to the absorbed microwave power (Q_v [J/(s m^3)]); and 4) heat exchange mechanism due to blood perfusion, proportional to the difference between blood and tissue temperature ($T_b - T$) (B [J/(s · °C · m^3)]).

To solve (2), the external surface of the body is bounded applying the convective boundary condition [23], obtained imposing the continuity of the heat flow perpendicular to the surface of the body (heat reaching this surface from the interior of the body through conduction must equal heat exchanged through convection with the surrounding medium or fluid)

$$-K\left(\frac{\partial T}{\partial n}\right)_S = H(T_s - T_e)\ [\mathrm{W/m^2}] \tag{3}$$

where: H [J/(m^2s °C)] is the convection coefficient, T_s is the surface temperature, and T_e is the fluid temperature.

To obtain a finite-difference formulation of the bioheat equation, the body under consideration is divided in cubic cells of δ size corresponding to those used in the FDTD method. Imposing the thermal balance to the (i, j, k) cell (the heat accumulated must equal the temperature increase in the cell multiplied by its thermal capacitance) [24], we obtain the following explicit equation:

$$\begin{aligned} T^{n+1}(i,j,k) &= \frac{K}{C\rho\delta^2}\,\delta t[T^n(i-1,j,k)+T^n(i+1,j,k) \\ &\quad + T^n(i,j-1,k)+T^n(i,j+1,k) \\ &\quad + T^n(i,j,k-1)+T^n(i,j,k+1)] \\ &\quad + T^n(i,j,k) \\ &\quad \cdot\left[1-\left(N_{\mathrm{INT}}\frac{K}{C\rho\delta^2}+N_{\mathrm{EXT}}\frac{H}{C\rho\delta}+\frac{B}{C\rho}\right)\delta t\right] \\ &\quad + N_{\mathrm{EXT}}\frac{H}{C\rho\delta}\,\delta t T_e + \frac{1}{C\rho}\,\delta t[Q_V(i,j,k)+A_0+BT_b] \end{aligned} \tag{4}$$

where N_{INT} and N_{EXT} are the number of internal and external nodes, respectively, adjacent to the cell (i, j, k). The first parenthesis of the previous expression only contains the temperatures of the internal nodes adjacent to the one considered and, therefore, is made up of less than six terms in the case of boundary nodes.

In order to avoid numerical instability, in the choice of the maximum size of the time step δt, the following criterion has to be followed:

$$\delta t \le \frac{1}{N_{\mathrm{INT}}\dfrac{K}{C\rho\delta^2}+N_{\mathrm{EXT}}\dfrac{H}{C\rho\delta}+\dfrac{B}{C\rho}}. \tag{5}$$

TABLE III
THERMAL PARAMETERS OF THE EYE'S TISSUES

Tissue	Spec. Heat (C) [J/kg °C]	Therm. Conduct. (K) [J/m s °C]
Humor	3997	0.603
Lens	3000	0.40
Sclera/Cornea	4178	0.58

The previous stability condition has been obtained on the basis of the approach suggested in [24]. Application of the criterion to the case of the eye gives rise to a maximum usable time step of approximately 0.4 s.

E. Thermal Parameters

When the thermal problem is applied to the eye, the bioheat equation can be solved by using the following simplifications:

1) the metabolic heat and the blood flow are absent;
2) part of the external surface of the eye (sclera) is strongly perfused: this means that a strong convective heat exchange is present on this surface;
3) the orbital fat has a low thermal conductivity and the heat exchanged by the eye through conduction with surrounding tissues is, therefore, negligible.

As a consequence of 1), the B and A_0 terms in the bioheat equation are negligible. As a consequence of 2) and 3), the eye is considered thermally isolated from the head, and two convective boundary conditions, taking into account the heat exchange with blood on the sclera and air on the cornea are used.

The values used for the physical parameters of the eye, based on those reported in the works by Lagendijk [25] and Scott [26], are given in Table III.

Lagendijk and Scott have also evaluated the convective coefficients to be applied on the surface of sclera and cornea. The values are $H_S = 65$ W/(m^2 °C) for the sclera, and $H_C = 20$ W/(m^2 °C) for the cornea.

It must be noted that the H_C coefficient takes into account three mechanisms: evaporation of the tear film, convective exchange with the air, and radiative exchange with the surrounding objects.

III. RESULTS

A. Validation

In order to validate the algorithms used for SAR and temperature evaluation, we have considered the exposure of a muscle cylinder ($\varepsilon_r = 47$, $\sigma = 2.21$ S/m, $\rho = 1070$ kg/m^3, $C = 3140$ J/(kg · °C), $K_m = 0.502$ J/(m · s · °C), $H = 8.37$ J/(m^2 · s · °C), $A_0 = 1005$ J/(m^3 · s), $B = 1674$ J/(m^3s · °C), $T_e = 24$ °C, $T_b = 37$ °C) to a plane wave (E parallel to the cylinder axis) with a frequency of 2.45 GHz and an incident power density of 100 mW/cm^2. The results have been compared with those obtained using the analytical solution [23].

Fig. 2(a) and (b) shows SAR and temperature distribution, respectively, along the diameter of the cylinder. In particular, the temperature distribution is shown at different instants of time computed from the beginning of the exposure. The numerical results are in good agreement with the analytical ones.

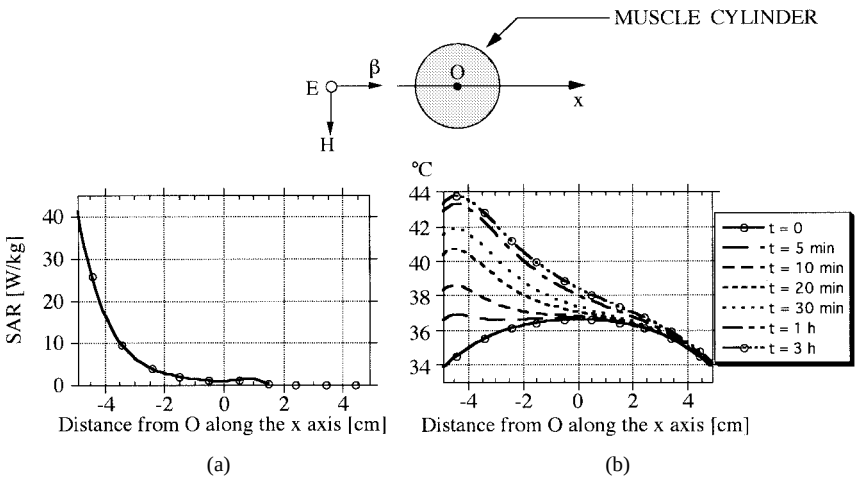

(a) (b)

Fig. 2. SAR and temperature distributions in an irradiated muscle cylinder (dots represent values from the analytical solution). (a) SAR distribution. (b) Temperature distributions.

TABLE IV
SAR_{MAX} INSIDE THE EYE COMPUTED USING DIFFERENT TWO-DIMENSIONAL MODELS

Frequency [GHz]	Eye Alone SAR_{MAX} [W/kg]	Eye with Nose SAR_{MAX} [W/kg]	Whole Head SAR_{MAX} [W/kg]
6	1.85	2.42	2.44
18	12.29	21.60	21.44
30	18.84	20.58	20.76

TABLE V
$SAR_{average}$ VALUES INSIDE THE EYE COMPUTED USING DIFFERENT TWO-DIMENSIONAL MODELS

Frequency [GHz]	Eye Alone $SAR_{average}$ [W/kg]	Eye with Nose $SAR_{average}$ [W/kg]	Whole Head $SAR_{average}$ [W/kg]
6	0.25	0.22	0.22
18	0.14	0.16	0.16
30	0.12	0.12	0.12

B. SAR Distribution in the Two-Dimensional Model

Since a three-dimensional model of the whole head requires a great amount of memory and computation time, we have first studied the interaction of a plane wave with the head by using a two-dimensional model.

These preliminary two-dimensional computations have been aimed at the evaluation of the minimum portion of the head around the eye to be considered in order to keep the model truncation error at an acceptable level.

For this reason, three different models have been considered: the first one is made up of a layer, extracted from the head, and including the eye and some cells of surrounding tissues (isolated eye), the second has been obtained by extracting from the head a layer including the eye and nose (eye with nose), the last considers the whole head layer. The results obtained with the three models are given in Tables IV and V with reference to SAR_{MAX} and SAR averaged over the eye ($SAR_{average}$), respectively. The Tables show that in the eye with nose model, SAR values are very close to those obtained with the whole head, while the results obtained using the isolated eye model are affected by a noticeable error, particularly with regard to SAR_{MAX}.

Analysis of Table IV indicates that the anatomical structure most influencing the maximum SAR inside the eye is the nose. In fact, scattering and reflections from the nose give rise to a focalizing effect. As a consequence of this focalization, SAR_{MAX} increases when the nose is included in the anatomical model.

Table V shows that the presence of the nose does not considerably influence the average SAR. This is due to the fact that at 6 GHz, a lateral penetration of the field, reaching the eye, is present. This field, penetrating from the truncated sides of the anatomical model, increases the SAR absorption inside the eye, compensating for the absence of the focalizing effect of the nose. At 18 and 30 GHz, the field penetrating laterally is absorbed in the few tissue cells surrounding the eye so that the average SAR is about the same, independent from the model.

On the basis of the previous observations, in the three-dimensional simulations, we have used a model of the eye which includes the nose and is large enough to prevent the field penetration from the sides of the eye.

C. Effect of Glasses

Some two-dimensional simulations have been performed to evaluate the effect of a glass lens, located in front of the cornea, on the SAR levels absorbed in the eye. As a dielectric slab located in front of a body can act as an adapter, it is possible that the presence of the lens results in an increased power absorption in the eye.

In order to find the distance of the glass lens [$\varepsilon_r = 5$; $\sigma = 0$] from the eye (chosen in the 1–2-cm range) and the lens thickness (in the 2–5-mm range), which could maximize the power absorbed in the eye, a simple unidimensional (layered) model of the structure has been considered and analyzed using microwave computer-aided design (CAD) software Touchstone.

The values obtained are shown in Table VI, together with the fraction of incident power transmitted in the cornea with and without lens.

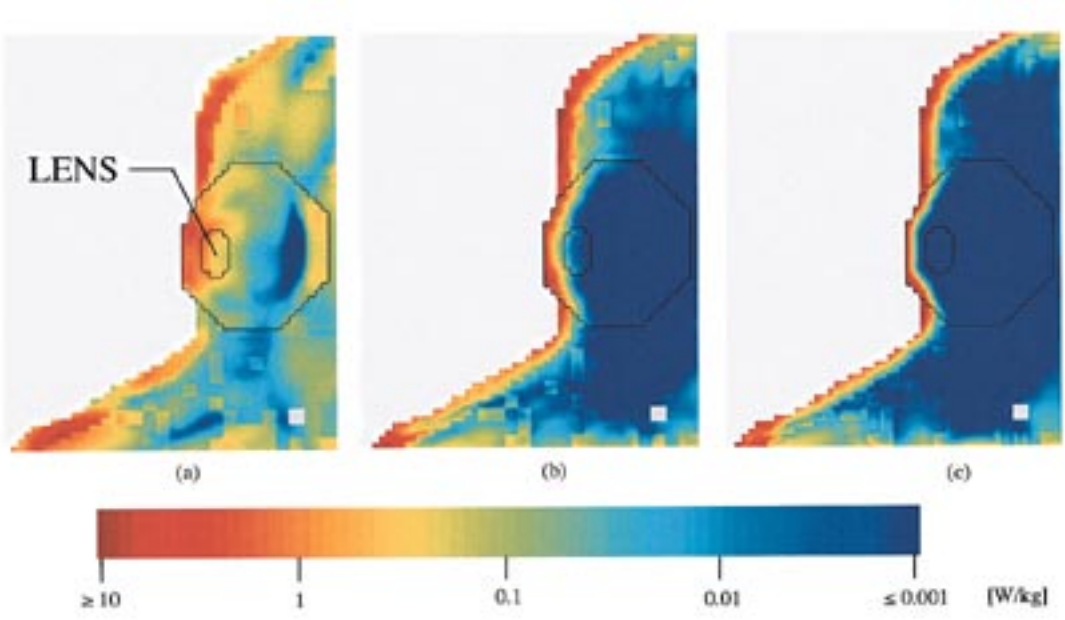

Fig. 3. SAR distributions in the three-dimensional eye model irradiated with 1 mW/cm^2. (a) $f = 6$ GHz. (b) $f = 18$ GHz. (c) $f = 30$ GHz.

TABLE VI
VALUES FOR THE GLASS-LENS THICKNESS AND POSITION PRODUCING THE HIGHEST POWER TRANSMITTED IN THE CORNEA

			Fraction of incident power transmitted in the cornea	
Frequency [GHz]	Thickness [mm]	Distance [cm]	Without lens	With lens
6	2	1	0.46	0.32
18	2	1.65	0.49	0.99
30	3.5	1.5	0.52	1

TABLE VII
SAR VALUES IN THE THREE-DIMENSIONAL EYE MODEL

Frequency [GHz]	SAR_{MAX} [W/kg]	$SAR_{average(eye)}$ [W/kg]	$SAR_{average(lens)}$ [W/kg]
6	6.317	0.253	0.594
18	36.558	0.107	0.009
30	40.414	0.068	0.000

The table shows that at the frequency of 6 GHz, the glass lens induces a decrease in the power absorption, mainly because of the reduced dimensions of the lens and the air gap compared to wavelength. At 18 and 30 GHz, a lens of appropriate thickness and position can almost perfectly match the cornea to the air (see Table VI).

Using the values obtained with the monodimensional study, we have performed some two-dimensional simulations on the whole head model placing a slab of glass before the eye. The obtained results differ from those of the monodimensional study as the frequency increases. This is because at high frequencies, the wavelength becomes comparable with the dimensions of the eye and the monodimensional model is no longer applicable. Notwithstanding these limitations, using the distance and width values obtained with the layered model, we have obtained at the frequency of 18 GHz, and with the two-dimensional model, an increase in the SAR averaged over the whole eye of approximately 31%.

TABLE VIII
TEMPERATURE VALUES AND HEATING INDUCED INSIDE THE THREE-DIMENSIONAL EYE MODEL. INCIDENT POWER 1-mW/cm^2 VERTICAL ELECTRIC FIELD

Frequency [GHz]	$T_{MAX(eye)}$ [°C]	$T_{MAX(cornea)}$ [°C]	$T_{MAX(lens)}$ [°C]	$\Delta T_{MAX(cornea)}$ [°C]	$\Delta T_{MAX(lens)}$ [°C]
no rad.	36.98	36.29	36.80	-	-
6	36.99	36.33	36.82	0.05	0.04
18	36.98	36.32	36.81	0.06	0.03
30	36.98	36.31	36.81	0.03	0.02

It must be noted that the unidimensional model is not an accurate representation of the realistic situation and it is possible that other values of the lens thickness and distance from the cornea result in even worse absorption conditions.

D. SAR Distribution in the Three-Dimensional Eye Model

After the preliminary two-dimensional simulations, we have performed SAR calculations on the more realistic three-dimensional eye model, assuming an incident wave having a power density of 1 mW/cm^2, equal to the most stringent limit found in the safety standards previously examined. The computed values are reported in Table VII, which shows maximum and average SAR values in the whole eye and SAR averaged over the lens alone.

The results show the way SAR changes with frequency. As frequency increases, $\mathrm{SAR_{MAX}}$ reaches higher values while, at the same time, the average SAR decreases. This is because, at higher frequencies, ε_r decreases and σ increases. The decrease of ε_r results in a better matching between the tissues and the air, with a higher fraction of the incident power entering the eye. The increase of σ causes this power to penetrate at a lower depth. The combined effect of these two mechanisms results in an increase of the $\mathrm{SAR_{MAX}}$ on the external surface of the eye (cornea) and in a contemporaneous decrease in SAR value averaged over the whole eye. The reason why the $\mathrm{SAR_{MAX}}$

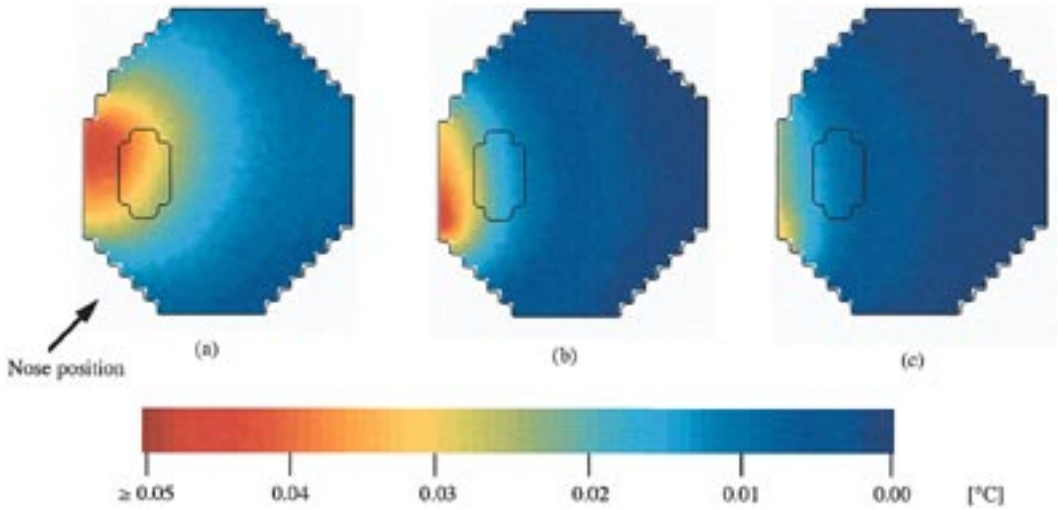

Fig. 4. Heating distributions in the three–dimensional eye model irradiated at 1 mW/cm^2. (a) $f = 6$ GHz. (b) $f = 18$ GHz. (c) $f = 30$ GHz.

remains almost unchanged passing from 18 to 30 GHz (see Table VII) has to be searched in the effect of the nose, which has a higher focalizing effect at 18 GHz.

Table VII also shows that at the higher frequencies (18 and 30 GHz), the eye lens is negligibly reached by the microwave power, thanks to the superficial absorption.

SAR distributions computed in the three-dimensional model are shown in Fig. 3(a)–(c) for the three frequencies of 6, 18, and 30 GHz, respectively. The figure refers to a horizontal section at the eye center.

The analysis of the distribution at 6 GHz [see Fig. 3(a)] shows that absorption takes place mainly in the part of the eye opposite to the nose; this is the consequence of the scattering by the nose itself. The distributions referring to the frequencies of 18 [see Fig. 3(b)] and 30 GHz [see Fig. 3(c)] show a SAR hot spot near the nose, due to its reflecting effect that focalizes the field.

E. Heating Induced in the Three-Dimensional Model

Thermal analysis has been performed in two steps: first of all, we have used the thermal model to evaluate the temperature distribution in a nonirradiated human eye; starting from this initial situation, we have calculated the temperature increase induced by the incident microwave radiation using the SAR values previously computed. During the thermal analysis an ambient temperature of 24 °C has been assumed.

The results of thermal simulations, assuming an incident power density of 1 mW/cm^2, are reported in Table VIII. The table shows the maximum temperatures reached in various parts of the eye and the maximum temperature increase found in the cornea and lens. Due to the low incident power levels and to the small volume subject to heating (superficial absorption), the heating process has reached steady state after approximately 7 min.

Analysis of data reported in Table VIII shows that the heating induced inside the eye by an incident power density of 1 mW/cm^2 at the frequencies under study is minimal, both in the lens and cornea.

It is interesting to note that the maximum temperature increase in the eye has been obtained using the frequency of 18 GHz. This is due to the fact that, at this frequency, $\mathrm{SAR_{MAX}}$ is high and the radiation is able to reach a penetration depth which is sufficient to heat the eye in the inner part and not only on its external layer, which is in direct contact with the air.

Instead, at 30 GHz, although the peak SAR is even higher, the penetration depth is too small to increase the temperature in an appreciable manner.

It is important to note that with respect to the lens, which is the part of the eye most sensitive to heating, the most dangerous frequency among those examined is 6 GHz. However, it has to be noted that at the frequencies of 18 and 30 GHz, although SAR dissipated in the lens is negligible, the lens is subject to a certain amount of heating due to the heat-conduction mechanism. Consequently, even at these frequencies, the lens remains the part of the eye most at risk.

Heating profiles computed in the eye at the three frequencies tested are shown in Fig. 4, with reference to the horizontal central section of the model.

These profiles indicate the different characteristics assumed by power absorption and heating in the eye. In particular, it can be noted how heating becomes more superficial as we move toward higher frequencies. However, thanks to the heat conduction mechanism, the heating process extends to a greater depth than that reached by SAR, as can be verified comparing the heating profiles with SAR distributions in Fig. 3.

The thermal profile relative to the frequency of 6 GHz [see Fig. 4(a)] shows that heating is maximum in the part of the eye opposite to the nose. Temperature distributions at 18 [see Fig. 4(b)] and 30 GHz [see Fig. 4(c)] instead show a temperature hot spot in a zone located near the nose.

Comparison between heating profiles and SAR distributions shows that in all three cases, the maximum temperature increase is located in the same zone as the peak SAR. This is mainly due to the fact that the blood flow is absent inside the eye.

IV. Conclusions

On the basis of the results obtained, it appears that the use of the exposure limits proposed by the different protection organizations we considered gives rise to temperature increases in the eye, which are far from inducing lens opacification.

Anyhow, some interesting considerations can be done, especially with reference to the CENELEC and IEEE/ANSI guidelines.

Using the reference level of 1 mW/cm^2 indicated in the CENELEC standard, the heating threshold of 0.3 °C in the eye lens is never reached. However, applying the local SAR limit (2 W/kg over 10 g of tissue) to the eye (which has a mass little inferior to 10 g) temperature increases induced in the lens at the frequencies of 18 and 30 GHz reach values around 0.6 °C, which corresponds to one-fifth of the threshold for the induction of cataract (3 °C).

As to the IEEE/ANSI standard, the use of an incident power density of 10 mW/cm^2 would result in a temperature increase in the lens greater than 0.3 °C both at 6 and at 18 GHz. Moreover, an incident power density of 10 mW/cm^2 at the frequency of 18 GHz would be able to induce heating greater than 0.5 °C in the cornea.

The adoption of a basic limit directly involving the temperature increase with different reference levels for the various parts of the body according to their sensitivity to heating could be more appropriate than the basic limit on average SAR currently used. In fact, our study has shown that with the same SAR value, as averaged over the whole eye, different heating is obtained when frequency varies. This is due to the fact that heating is influenced not only by the mean power absorbed in a certain volume of the tissue, but also by the way in which the SAR is distributed in the volume.

References

[1] K. Pahlavan and A. H. Levesque, "Wireless data communications," *Proc. IEEE*, vol. 82, pp. 1398–1430, Sept. 1994.

[2] H. H. Meinel, "Commercial applications of millimeter-wave history, present status, and future trends," *IEEE Trans. Microwave Theory Tech.*, vol. 43, pp. 1639–1695, July 1993.

[3] C. H. Durney, "The physical interactions of radio-frequency radiation fields and biological systems," *AGARD Lecture Series*, no. 138, pp. 2.1–2.19, 1985.

[4] S. Baranski and P. Czerski, *Biological Effects of Microwaves.* Stroudsburg, PA: Dowden, 1976, pp. 146–149.

[5] A. W. Guy, J. C. Lin, P. O. Kramar, and A. F. Emery, "Effect of 2450 MHz radiation on the rabbit eye," *IEEE Trans. Microwave Theory Tech.*, vol. MTT-23, pp. 492–498, June 1975.

[6] B. Appleton, S. E. Hirsch, and P. V. K. Brown, "Investigation of single-exposure microwave ocular effects at 3000 MHz," *Annals New York Academy Sci.*, vol. 247, pp. 125–134, 1975.

[7] O. P. Gandhi and A. Riazi, "Absorption of millimeter waves by human beings and its biological implications," *IEEE Trans. Microwave Theory Tech.*, vol. MTT-34, pp. 228–235, Feb. 1986.

[8] D. H. Sliney and B. E. Stuck, "Microwave exposure limits for the eye: Applying infrared laser threshold data," in *Radiofrequency Radiation Standards.* New York: Plenum, 1994, pp. 79–87.

[9] P. R. Wainwright and M. J. Whillock, "Measurements and mathematical models in the assessment of optical radiation hazards to the eye," *J. Radiological Protection*, vol. 10, no. 4, pp. 263–269, 1990.

[10] A. Taflove and M. E. Brodwin, "Computation of the electromagnetic fields and induced temperatures within a model of the microwave irradiated human eye," *IEEE Trans. Microwave Theory Tech.*, vol. MTT-23, pp. 888–896, June 1975.

[11] *IEEE Standard for Safety Levels with Respect to Human Exposure to radio Frequency Electromagnetic Fields, 3 kHz to 300 GHz*, IEEE Standard C95.1-1991, 1992.

[12] IRPA Guidelines, "Guidelines on limits of exposure to radiofrequency electromagnetic fields in the frequency range from 100 kHz to 300 GHz," *Health Phys.*, vol. 54, no. 1, pp. 115–123, 1988.

[13] *Human Exposure to Electromagnetic Fields. High Frequency (10 kHz to 300 GHz)*, European Communities Prestandard ENV 50166-2, 1995.

[14] P. Bernardi, M. Cavagnaro, and S. Pisa, "Assessment of the potential risk for humans exposed to millimeter-wave wireless LANs: The power absorbed in the eye," *Wireless Networks*, vol. 3, no. 6, pp. 511–517, 1997.

[15] ——, "Evaluation of the power absorbed in human eyes exposed to millimeter waves," in *Int. Symp. Electromagn. Compat.*, Rome, Italy, Sept. 1996, pp. 194–199.

[16] A. Taflove, *Computational Electrodynamics: The Finite-Difference Time-Domain Method.* Norwood, MA: Artech House, 1995.

[17] K. S. Kunz and R. J. Luebbers, *The Finite Difference Time Domain Method for Electromagnetics.* Boca Raton, FL: CRC Press, 1993.

[18] M. C. Steel and R. J. Sheppard, "Dielectric properties of lens tissue at microwave frequencies," *Bioelectromagnetics*, vol. 7, pp. 73–81, 1986.

[19] J. L. Schepps and K. R. Foster, "The UHF and microwave dielectric properties of normal and tumor tissue: Variation in dielectric properties with tissue water content," *Phys. Medicine and Biology*, vol. 25, no. 6, pp. 1149–1159, 1980.

[20] C. Gabriel, R. J. Sheppard, and E. H. Grant, "Dielectric properties of ocular tissues at 37°C," *Phys. Medicine and Biology*, vol. 28, no. 1, pp. 43–49, 1983.

[21] M. A. Stuchly, A. Kraszewski, S. Stuchly, and A. M. Smith, "Dielectric properties of animal tissues in vivo at radio and microwave frequencies: Comparison between species," *Phys. Medicine and Biology*, vol. 27, no. 7, pp. 927–936, 1982.

[22] S. Gabriel, R. W. Lau, and C. Gabriel, "The dielectric properties of biological tissues—III: Parametric models for the dielectric spectrum of tissues," *Phys. Medicine and Biology*, vol. 41, pp. 2271–2293, 1996.

[23] F. Bardati, G. Gerosa, and P. Lampariello, "Temperature distribution in simulated living tissues irradiated electromagnetically," *Alta Frequenza*, vol. XLIX, no. 2, pp. 61–67, 1980.

[24] N. Ozisik, *Heat Transfer: A Basic Approach.* New York: McGraw-Hill, 1985.

[25] J. J. W. Lagendijk, "A mathematical model to calculate temperature distributions in human and rabbit eyes during hypertermic treatment," *Phys. Medicine and Biology*, vol. 27, no. 11, pp. 1301–1311, 1982.

[26] J. A. Scott, "A finite element model of heat transport in the human eye," *Phys. Medicine and Biology*, vol. 33, no. 2, pp. 227–241, 1988.

Paolo Bernardi (M'66–SM'73–F'93) was born in Civitavecchia, Italy, in 1936. He received the degree in electrical engineering and the *Libera Docenza* degree in microwaves from the University of Rome, Rome, Italy, in 1960 and 1968, respectively.

Since 1961, he has been with the Department of Electronics, University "La Sapienza" of Rome, Rome, Italy, where he became a Full Professor in 1976, and was Director of the department from 1982 to 1988. His research work has dealt with the propagation of EM waves in ferrites, microwave components, biological effects of the EM waves, and EM compatibility. He has authored over 140 scientific papers and numerous invited presentations at international workshops and conferences. He is currently Project Coordinator of the European community project CEPHOS, which is devoted to the EM dosimetry for cellular phones. He was chairman of Commission K "Electromagnetics in Biology and Medicine" of the International Union of Radio Science (1993–1996), chairman of a Commission of the Italian National Research Council (CNR), where he worked on the "National Project" on electromagnetic compatibility in electrical and electronic systems, and vice-chairman of the European Community COST Project 244 on biomedical effects of electromagnetic radiation (1993–1997). He is an associate editor for the URSI Radio Science Bulletin. He is a member of the Editorial Board for *Microwave and Optical Technology Letters*. He was the Guest Editor of a special issue of *Alta Frequenza* (March 1980) on nonionizing EM radiation, and of a special issue of *Wireless Networks* (December 1997) on exposure hazards and health protection in personal communication services.

Dr. Bernardi is member of the BEMS, EBEA, and Socio Fedele of the Italian Electrical and Electronic Society (AEI). He is a member of the Editorial Board for IEEE Microwave and Guided Wave Letters. From 1979 to 1980, he was the chairman of the IEEE Middle and South Italy Section. In 1984, he was awarded the IEEE Centennial Medal.

Marta Cavagnaro was born in Rome, Italy, in 1966. She received the *cum laude* degree in electronic engineering and the Ph.D. degree from the University "La Sapienza" of Rome, Rome, Italy, in 1993, and 1997, respectively. In 1993, she gained a scholarship from Alenia Spazio S.p.A. to study the coupling between EM fields and triaxial cables and, in the same year, she began the Ph.D. course in electronic engineering at the University "La Sapienza" of Rome, receiving the Ph.D. degree in 1997.

Her current research interests are dosimetric aspects of the interaction between EM fields and biological systems and numerical techniques.

Dr. Pisa was the recipient of the 1996 URSI Young Scientist Award.

Stefano Pisa (M'91) was born in Rome, Italy, in 1957. He received the electronic engineering and Ph.D degrees from the University "La Sapienza" of Rome, Rome, Italy, in 1985 and 1988, respectively.

He is currently with the Department of Electronics, University "La Sapienza" of Rome, as a Researcher. His research interests are in the interaction between EM fields and biological systems and in therapeutic and diagnostic applications of EM fields.

Emanuele Piuzzi was born on May 25, 1972, in Lecce, Italy. He received the *cum laude* degree in electronic engineering from the University "La Sapienza" of Rome, Rome, Italy, in 1997, and is currently working toward the Ph.D. degree.

He is currently studying hybrid techniques for the solution of Maxwell's equations, with particular attention to those involving FDTD. His current research interests are radiofrequency dosimetry, heating induced inside human beings exposed to RF and microwave fields, and hybrid numerical techniques for EM-field computation.